Direct observation of He$^+$ pick-up ions of interstellar origin in the solar wind

E. Möbius*, D. Hovestadt*, B. Klecker*, M. Scholer*, G. Gloeckler† & F. M. Ipavich†

* Max-Planck-Institut für Physik und Astrophysik, Institut für extraterrestrische Physik, 8046 Garching, FRG
† Department of Physics and Astronomy, University of Maryland, College Park, Maryland 20742, USA

Singly-ionized helium with a velocity distribution extending up to double the solar wind velocity has been detected in interplanetary space. This distribution unambiguously determines the source: interstellar neutrals, ionized and accelerated in the solar wind. The observed significant flux increase in early December is due to the gravitational focusing of the interstellar neutral wind on the downwind side of the Sun.

THE penetration of the interstellar medium into the heliosphere and the interaction between the solar wind and the interstellar gas have been of great interest for many years[1-4]. The first experimental evidence of neutral interstellar hydrogen penetrating into the heliosphere was obtained from Lyman α sky background mapping[5,6]. Similar observations of interstellar helium using the He I 584-Å resonance line[7-9] revealed the existence of an interstellar neutral wind in interplanetary space which is subjected to the forces of solar gravitation and radiation pressure. When approaching the Sun, the interstellar gas is ionized by solar ultraviolet radiation, by charge exchange with solar wind ions and by collisions with solar wind electrons. The newly created ions are then picked up by the solar wind through interaction with the interplanetary magnetic field.

While most of the constituents are already ionized far beyond the orbit of the Earth, neutral helium (because of its high ionization potential) approaches the Sun to <1 AU (ref. 1). Therefore, a significant fraction of the helium is ionized inside the Earth's orbit and one would expect that these ions are observable by spacecraft in the solar wind. So far, no conclusive measurement on He$^+$ ions of interstellar origin has been given. Although signatures of He$^+$ in the solar wind with varying abundances have been reported occasionally[10,11], a systematic search for a permanently present flux of interstellar He$^+$ as part of the solar wind resulted only in upper limits more than one order of magnitude below the estimated flux levels[12]. After this negative result Vasyliunas and Siscoe[13] suggested that the newly created He$^+$ ions may not be thermalized rapidly enough to occur within the solar wind distribution. The expected broad energy and angular distribution of the interstellar helium ions, however, was not visible to the particle detectors flown on spacecraft up to now. A search for interplanetary He II emission at 304 Å was also not conclusive[14]. In this article, we will report measurements with a time-of-flight (TOF) spectrometer in which the interstellar helium ions and their velocity distribution in the solar wind are clearly identified for the first time.

Instrumentation and spacecraft

The data presented here were obtained with the SULEICA (Supra-thermal Energy Ionic Charge Analyser) instrument of the Max-Planck-Institut and the University of Maryland onboard the IRM spacecraft of the AMPTE (Active Magnetospheric Particle Tracer Explorer) project. The IRM was launched on 16 August 1984, into a highly elliptical orbit with an apogee of 18.6 R_E. During the time period from launch until December 1984 the satellite spent a large fraction of each orbit in the solar wind upstream of the Earth's bow shock.

The SULEICA instrument combines the selection of incoming ions according to their energy per charge by electrostatic deflection with a subsequent TOF analysis and the final measurement of the residual ion energy in a silicon surface barrier detector. The energy range from 5 to 270 keV/charge is covered by stepping the analyser voltage in 24 logarithmically spaced voltage steps in synchronism with the spacecraft spin. The fan-like
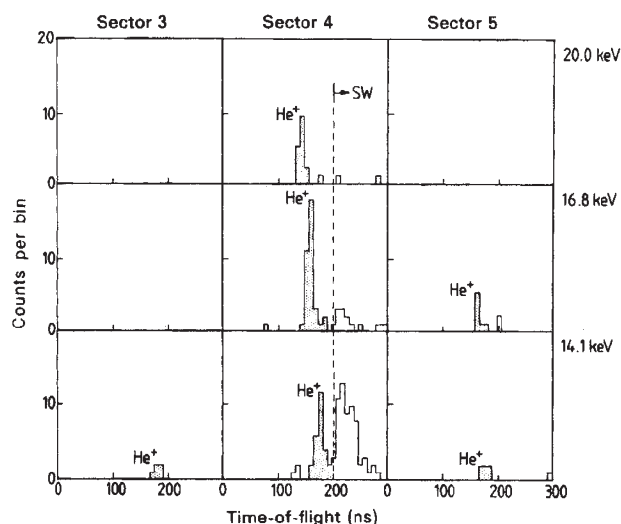

Fig. 1 Typical TOF-histograms at three different energy steps taken in the Sun sector and the two adjacent sectors. The data were obtained during a period of 45 min on 11 November 1984, at ~18 R_E in front of the Earth's bow shock.

aperture of the electrostatic analyser (two concentric segments of a sphere) covers a solid angle of 10° in azimuth and 40° in elevation symmetric to the plane perpendicular to the spacecraft spin axis. The directional information in azimuth is provided by a sectoring scheme with 16 sectors for protons and α particles and eight sectors for the other ions. The geometrical factor of the instrument is 4.3×10^{-2} cm^2 sr and its energy resolution is $\Delta E/E \approx 0.097$. A more detailed description may be found elsewhere[15].

The expected energy of the pick-up ions (≤ 40 keV) is too low to create energy signals significantly above the noise level of the solid state detectors. Therefore, the ion species are identified by combining the electrostatic deflection (E/Q) and the TOF signal. For each specific E/Q step, the TOF distribution represents a unique mass-per-charge distribution, since $M/Q \sim E/Q \times$TOF^2. Recently this type of analysis has been successfully applied to identify Li$^+$ pick-up ions after the lithium vapour cloud releases of the AMPTE project in the solar wind[16].

Basic observations

For the present investigation a limited number (12) of observational periods in the solar wind were chosen between launch of the spacecraft and the end of December 1984. During all periods we observe a significant peak at $M/Q = 4$ in the TOF-histograms for E/Q steps which correspond to energies higher than we would expect for genuine singly charged solar wind helium. Depending on the E/Q step we also observe a broad and variable peak at TOF-values which correspond to the actual
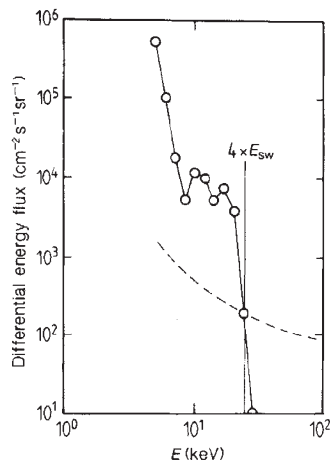
Fig. 2 Differential energy flux spectrum of the $M/Q = 4$ channel taken in the Sun sector with an accumulation time of 40 min. The dashed line represents the 1 count level for each energy.

Fig. 3 a, Cut through the fully developed velocity distribution of pick-up ions in the spin plane of the spacecraft (shaded area) along with the sectoring and voltage stepping scheme of the instrument. The velocity space element, which is used to determine the differential energy flux as seen by the instrument, is left blank. b, Similar representation in the solar wind frame. The velocity space element, over which the actual integration is performed, is left blank.

solar wind velocity. These ions with M/Q values well above 4 represent heavy ions of the solar wind. In addition, the signature of the He^+ ions at $M/Q = 4$ is also seen in the two sectors adjacent to the sunward direction. A typical example of TOF-histograms for three different voltage steps and all three azimuthal sectors with the He^+ peak is shown in Fig. 1. The sample was taken during a 45-min interval on 11 November 1984, when no energetic ions occurred upstream of the bow shock. Note, however, that the He^+ signature is visible at all orientations of the interplanetary magnetic field and is independent of whether or not upstream particles are present.

Figure 2 shows the differential energy flux spectrum of the He^+ ions in the Sun sector for the same time period. The spectrum is basically flat between ≈8 and 22 keV with a sharp cutoff at ~22.3 keV. This value corresponds to about four times the solar wind bulk energy of helium (indicated by the vertical line) for this time period. The actual solar wind velocity was 550 km s^{-1}, as derived from the data of the Max-Planck-Institut/University of California Berkeley three-dimensional-Plasma instrument on IRM[17]. Below 8 keV a sharp rise of the spectrum occurs which is attributed to solar wind ions with $M/Q = 4$, for example, Si^{7+} and S^{8+} (ref. 12). The dashed line in Fig. 2 indicates the one count limit for He^+.

Signature of pick-up ions

In contrast to genuine solar wind ions heavier than protons, which flow with almost solar wind bulk velocity, freshly created ions in interplanetary space are initially at rest. After ionization they are immediately subjected to the combined forces of the interplanetary $v_{sw} \times B$ electric field and the magnetic field B where v_{sw} is the solar wind velocity. In the inertial system (which coincides with the rest frame of the spacecraft), the ions initially perform a cycloidal motion perpendicular to the local magnetic field. The velocity varies between basically zero (the velocity of the neutral wind at ≈20 km s^{-1} is neglected compared with the solar wind velocity) and a maximum value

$$v_{\perp max} = 2\, v_{sw} \sin \alpha \qquad (1)$$

which is determined by the solar wind velocity and the angle α between its flow direction and the local magnetic field. The maximum energy of pick-up ions then is

$$E_{\perp max} = 4(M/2)v_{sw}^2 \sin^2 \alpha \qquad (2)$$

In the solar wind frame, the pitch angle distribution of these particles is a ring in velocity space with the pitch angle α, that is, the ions gyrate with $v_\perp = v_{sw} \sin \alpha$ and move along the magnetic field with $v_\parallel = v_{sw} \cos \alpha$. Observations of artificially-injected lithium in the solar wind which have been made within the first cycloid after the ionization are compatible with such
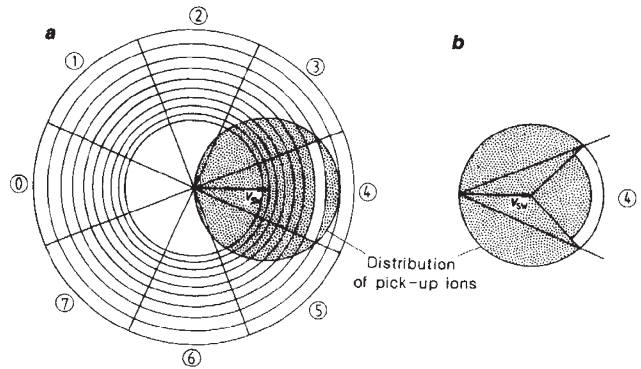
an undisturbed pick-up distribution[16]. Our observations of He^+ ions, which are spread over a large volume in velocity space, seem to indicate a significant broadening of the initial ring distribution in pitch angle as well as in energy.

Cosmic rays are strongly pitch-angle-scattered by magnetic field fluctuations in the solar wind, while their energy remains almost unaffected[18]. The corresponding mean free path for scattering of He^+ pick-up ions (with a typical magnetic rigidity of 5-10 MV) turns out to be about 0.05 AU according to a compilation of cosmic-ray propagation parameters[19]. From these arguments, pitch angle scattering seems to be rather efficient for pick-up ions, and shortly after ionization a spherical shell distribution in velocity space is formed within the rest frame of the solar wind. Initially, the ions are injected into the solar wind with the energy $E_0 = (M/2)v_{sw}^2$ (with velocity components $v_\parallel$ and $v_\perp$ as discussed above). Therefore, the radius of the spherical shell distribution is equal to the solar wind velocity. Subsequently, the ion energy decreases as a result of adiabatic deceleration during the radial transport with the expanding solar wind. Due to adiabatic deceleration the energy of fully pitch-angle-scattered particles varies like

$$E/E_0 = \left(\frac{r_i}{r}\right)^{4/3} \qquad (3)$$

with the distance r from the Sun, starting at the location of birth of the ion r_i (ref. 13). This relation immediately leads to a mapping of the spatial source distribution of pick-up ions upstream of the spacecraft into an energy or velocity distribution in the solar wind frame at the location of the satellite which can be written as:

$$f(v) = \frac{3 N_0\, v_{ion}\, r_0}{8 \pi\, v_{sw}^4} \left(\frac{v}{v_{sw}}\right)^{-3/2} \qquad (4)$$

N_0 and v_{ion} are the neutral density and the ionization rate of the interstellar gas at the Earth's orbit ($r_0 = 1$ AU). v_{ion} is assumed to vary like $1/r^2$ with the intensity of solar ultraviolet radiation. In the spacecraft frame of reference, this results in a particle distribution which extends between $E = 0$ and a maximum energy

$$E_{max} = 4E_{sw} = 4(M/2)v_{sw}^2 \qquad (5)$$

for particles coming from the sunward direction. Such a distribution with a more or less flat spectrum in differential energy flux is, indeed, observed between about 8 and 22 keV (see Fig. 2).

From these observations, it can be concluded that the velocity distribution of the pick-up ions is basically a full sphere centred at the solar wind velocity. A cut through this distribution in the plane perpendicular to the spin axis of the satellite is shown in Fig. 3. The azimuthal sectoring scheme and the voltage stepping
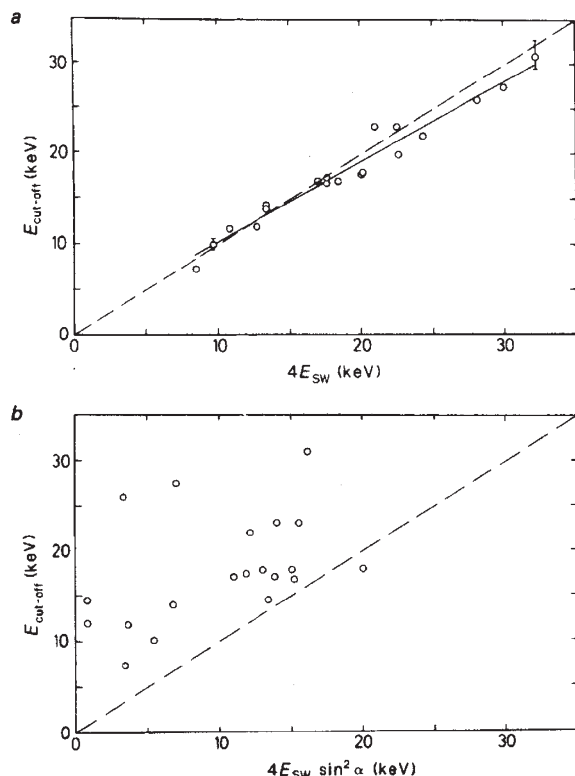
a

b

Fig. 4 Correlation of the experimental cutoff energies of the He^+ spectrum with the fourfold solar wind bulk energy $4\,E_{SW}$ of helium (a) and with the maximum pick-up energy perpendicular to the interplanetary magnetic field $4\,E_{SW}\sin^2\alpha$ (b).

scheme (concentric circles) are overlayed. This interpretation is also supported by the TOF histograms shown in Fig. 1, where the He^+ peak is observed in the Sun sector 4 as well as in the neighbouring sectors 3 and 5. The energy spectrum displayed in Fig. 2 represents a cut through the distribution in the Sun sector. It follows from the measured flat energy spectrum that a large fraction of the sphere in velocity space rather than only the outer shell is filled with He^+ ions. Otherwise, a significant flux decrease between E_{sw} and $4\,E_{sw}$ would be expected. Therefore, a significant part of the He^+ population originates from locations several tenths of an AU upstream of the spacecraft. The energy of these ions has decreased on their way according to relation (3).

The energy spectra of the He^+ ions have been investigated for several time periods of different solar wind velocities and interplanetary magnetic field directions. In Fig. 4, the observed cutoff energies E_{cutoff} (defined by a decrease of the differential energy flux by a factor of 10 compared with the mean plateau level) are plotted first against the fourfold solar wind bulk energy $4\,E_{sw}$ of helium as given by relation (5) and second against the initial maximum pick-up energy $4\,E_{sw}\sin^2\alpha$ according to relation (2). There is an excellent correlation with the full four-fold solar wind energy (correlation coefficient 0.98), while the correlation with the maximum pick-up energy is very poor (correlation coefficient 0.36). This result clearly indicates that the pick-up ions in all conditions have mainly lost their directional information due to pitch angle scattering and that most of the ions originate from regions beyond one mean free scattering length (0.05 AU) upstream of the observer.

Note that the generation of several types of plasma waves by the highly unstable distribution of pick-up ions has been discussed in the past[20,21]. These waves were expected to lead to a complete thermalization in energy of the pick-up ion distribution in the solar wind frame of reference in addition to pitch angle scattering. However, the results described above—in particular, the sharp cutoff in energy—indicate that the influence of these waves on the He^+ distribution can be neglected compared with the adiabatic cooling.
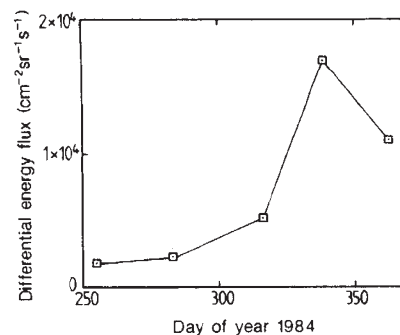

Fig. 5 Differential energy flux of 20-keV He^+ ions obtained in the Sun sector for five different time periods between September and December 1984.

Source of the He^+ ions

Knowing the velocity distribution of the He^+ ions as shown in Fig. 3, the source strength $S = N_0\,\nu_{ion}$ of the pick-up ions can be obtained from the measured differential energy flux at a fixed energy. The differential energy flux can be calculated by integrating the distribution function (relation (4)) over one voltage step and the Sun sector in the spacecraft frame (blank area in Fig. 3a). Instead of performing the full transformation from the solar wind frame into the spacecraft frame we use the fact that the distribution is isotropic in the solar wind frame and that near the maximum energy of the ion distribution (in the Sun sector) the volume element in velocity space $\Delta\Omega v^2\Delta v$ covered by one energy channel of the instrument appears to be extended by a factor of four in solid angle in the solar wind frame compared with the spacecraft frame as indicated in Fig. 3b. Within this approximation, the integration is performed over the corresponding sector in the solar wind frame (blank area in Fig. 3b). Using the distribution function (5) we obtain for the differential energy flux:

$$\frac{\Delta JE}{\Delta E} = \frac{3N_0\nu_{ion}r_0E}{8\pi\Delta\Omega\,\Delta E}\,4\Delta\Omega\,\frac{1}{v_{sw}^4}\int_{0.9v_{sw}}^{v_{sw}}\left(\frac{v}{v_{sw}}\right)^{-3/2}v^3\,dv \qquad (6)$$

According to the energy resolution of the instrument ($\Delta E/E \approx 0.1$, corresponding to $\Delta v/v \approx 0.05$) the integration limits in velocity are $0.9\,v_{sw}$ and v_{sw} in the solar wind frame. Note that the differential energy flux (compared with the differential particle flux $\Delta J/\Delta E$), when taken at the maximum energy of the pick-up distribution, does not vary with the solar wind velocity. Therefore, this quantity is a suitable parameter for subsequent long-time studies of the He^+ source. Using $w = v/v_{sw}$ we find:

$$\frac{\Delta JE}{\Delta E} = \frac{3}{2\pi}\,N_0\nu_{ion}r_0\,\frac{E}{\Delta E}\int_{0.9}^{1}w^{3/2}dw \approx 0.5\,N_0\nu_{ion}r_0 \qquad (7)$$

Taking an ionization rate $\nu_{ion} = 1.25\times10^{-7}\,s^{-1}$ at 1 AU (ref. 9) a value of $N_0r_0 = 1.2\times10^{11}\,cm^{-2}$ is derived from the mean differential energy flux between 16 and 20 keV ($7\times10^3\,s^{-1}\,cm^{-2}\,sr^{-1}$) on 11 November 1984. The actual column density upstream of the spacecraft corresponds to about half the value of N_0r_0.

Possible sources for singly charged ions which are injected into the solar wind with zero velocity are the interstellar neutral gas as discussed above and, in addition, planetary atmospheres and cometary comae. Of the latter ones the only source of interest for the observations reported here is the Earth's atmosphere. In contrast to the interstellar gas, which is present over a large scalelength in interplanetary space, the terrestrial sources of neutral helium are rather localized. Because the density of the exosphere typically varies like $1/R^2$ with distance from the Earth, the remaining scalelength of Earth's exosphere (the outer regime of the atmosphere) beyond the location of the spacecraft ($18\,R_E$) is of the order of $20\,R_E$. Therefore, a terrestrial origin can be ruled out for the observed He^+ ions for two reasons.

First, the observed velocity distribution can only be explained in terms of a source which extends far beyond the mean free

scattering length of ~0.05 AU upstream from the Earth, while the terrestrial exosphere has a scalelength of typically 20 R_E.

Second, with a scalelength of ~20 R_E the measured column density would lead to a helium density of ~5 cm^{-3} at a distance of 18 R_E. This value exceeds densities known for exospheric helium by more than 3 orders of magnitude[22].

Therefore, the observed He^+ ions are most likely of interstellar origin. The corresponding helium density in interplanetary space upstream of the spacecraft on 11 November was determined to be $N_0 \approx 8 \times 10^{-3}$ cm^{-3}.

The flux of He^+ ions and, therefore, the neutral density of helium shows a significant variation over the observation period from September to December 1984. In Fig. 5, the differential energy flux of He^+ at 20 keV is plotted against time. For this analysis, only those time periods were taken when the solar wind velocity exceeded 550 km s^{-1}; that is, the maximum energy E_{cutoff} was >20 keV. The differential energy flux is low in September and October (~2×10^3 s^{-1} cm^{-2} sr^{-1}). An increase by about a factor of 10 is observed until early December, after which the flux falls off again towards the end of December. This result is in good agreement with models of the spatial distribution of neutral helium in interplanetary space and the observations of He I 584-Å radiation[8,9]. During December, the Earth is on the downwind side of the interstellar neutral wind with respect to the Sun. Here the helium is supposedly focused by the gravitational forces of the Sun and, therefore, the local density is enhanced significantly. The observation of this effect constitutes additional evidence for the interstellar source of the He^+ ions.

These observations are of particular importance, since various parameters of the local interstellar medium can be derived from the annual variation of the flux of He^+ ions: (1) the location of the apex; (2) the value of the relative velocity between the sun and the local interstellar medium; (3) the temperature; and (4) the density of the interstellar helium.

The absolute value of the density near the Earth as given above is compatible with results reported from ultraviolet measurements[8,9]. A quantitative analysis of the density outside the heliosphere and the determination of the parameters of the local interstellar medium as listed under items (1) to (4) above requires a detailed comparison of the experimental results with theoretical models of the neutral helium distribution in the heliosphere. This is beyond the scope of the present paper and will be presented in future work.

Furthermore, these pick-up ions represent a source of ions with a velocity distribution clearly distinguishable from the solar wind. To study their subsequent acceleration at the Earth's bow shock and at interplanetary shocks will be of great interest. Finally, these ions are most likely the seed particles for the so-called anomalous component of cosmic rays for which an interstellar origin and subsequent acceleration in the interplanetary medium[24] or at the terminating shock of the heliosphere[25] has been proposed.

1. Axford, W. I. NASA SP-308, 609–660 (1972).
2. Fahr, H. J. Space Sci. Rev. 15, 483–540 (1974).
3. Holzer, T. E. Rev. Geophys. Space Phys. 15, 467–490 (1977).
4. Thomas, G. E. A. Rev. Earth planet. Sci. 6, 173–204 (1978).
5. Thomas, G. E. & Krassa, R. F. Astr. Astrophys. 11, 218–233 (1971).
6. Bertaux, J. L. & Blamont, J. E. Astr. Astrophys. 11, 200–217 (1971).
7. Paresce, F. & Bowyer, S. Astr. Astrophys. 27, 399–406 (1973).
8. Weller, C. S. & Meier, R. R. Astrophys. J. 193, 471–476 (1974).
9. Dalaudier, F., Bertaux, J. L., Kurt, V. G. & Mironova, E. N. Astr. Astrophys. 134, 171–184 (1984).
10. Bame, S. J., Hundhausen, A. J., Asbridge, J. R. & Strong, I. B. Phys. Rev. Lett. 20, 393–395 (1968).
11. Schwenn, R., Rosenbauer, H. & Mühlhäuser, K. H. Geophys. Res. Lett. 7, 201–204 (1980).
12. Feldman, W. C., Asbridge, J. R. & Bame, S. J. J. geophys. Res. 79, 1808–1812 (1974).
13. Vasyliunas, V. M. & Siscoe, G. L. J. geophys. Res. 81, 1247–1252 (1976).
14. Paresce, F., Fahr, H. J. & Lay, G. J. geophys. Res. 86, 10038–10048 (1983).
15. Möbius, E. et al. IEEE Trans. Geosci. Remote Sensing GE-23, 274–279 (1985).
16. Möbius, E. et al. J. geophys. Res. (in the press).
17. Paschmann, G. et al. IEEE Trans. Geosci. Remote Sensing GE-23, 262–266 (1985).
18. Jokipii, J. R. Rev. Geophys. Space Phys. 9, 27–87 (1971).
19. Mason, G. M. et al. Astrophys. J. 267, 844–867 (1983).
20. Wu, C. S. & Davidson, R. C. J. geophys. Res. 77, 5399–5406 (1972).
21. Hartle, R. E. & Wu, C. S. J. geophys. Res. 78, 5802–5807 (1973).
22. Paul, G. thesis, Univ. Bonn (1979).
23. Fahr, H. J. Space Res. 13, 837–842 (1973).
24. Fisk, L. A. Astrophys. J. 206, 333–341 (1976).
25. Pesses, M. et al. Astrophys. J. Lett. 246, L85–L88 (1981).

Axial processes along a segment of the East Pacific Rise, 10°–12° N

G. Thompson*, W. B. Bryan*, R. Ballard*, K. Hamuro† & W. G. Melson‡

* Woods Hole Oceanographic Institution, Woods Hole, Massachusetts 02543, USA
† Japanese Consulate, 600 Atlantic Ave, Boston, Massachusetts, USA
‡ Smithsonian Institution, Washington DC 20550, USA

Axial segments of the East Pacific Rise are made up of individual volcanoes. Each volcano has a distinct magma composition and shows a systematic variation in the fractional crystallization with distance along the axis from the central chamber. Hydrothermal venting, lava morphology and tectonics also vary along the axis. Lavas erupted near transform faults, from the tips of propagating rifts in overlapping spreading centres, and from near-axis seamounts have different and variable compositions.

MID-OCEAN ridge spreading centres have recently been shown to consist of discrete segments separated by transform faults and conjugate spreading centres (also called overlapping spreading centres (OSC) or non-transform offsets[1,2]). Typically, in each segment the axial depth shows a minimum or topographic high at some point between the two ends[1–4]. Francheteau and Ballard[4] have proposed that the topographic highs lie above the principal magma chambers feeding lavas to the axis and are thermal expressions of such chambers. Their model predicts that relative volumes of lava and morphology of lava flows should change systematically along the axis away from the topographic high. Specifically, pillow lavas should increase relative to sheet flows, fracturing should increase and hydrothermal activity should decrease along-ridge away from the topographic high. To date, observations supporting this hypothesis have been made at several locations of different spreading rates, but have been limited to a few kilometres along the axis in the vicinity of the axial topographic high.

We report here on our recent observations over a 180-km length of East Pacific Rise (EPR) axis between 10° and 12° N,